ESA Workshop on Optical Interferometry in Space

Granada, Spain, June 16-18 1987. ESA SP-273 (August 1987)

Pages 73-83

FIBER-LINKED TELESCOPE ARRAYS ON THE GROUND AND IN SPACE

P. Connes — CNRS, Service d'Aéronomie, Verrières, 91371, France

F. Roddier, S.Shaklan — NOAO-ADP, Box 2632, Tucson, AZ 85726, USA

E.Ribak — JPL, Pasadena CA 91109, USA

ABSTRACT/RESUME

The use of single-mode optical fibers in telescope arrays, first proposed at the Cargèse meeting for a set of free-flying spacecrafts, is further developed, and applied to more modest, shorter-range projects. The basic advantage remains a considerable simplification in the control system; the main limitation is spectral range, but much progress has already been made in IR fibers. Two proposals are described here: a ground-based array of small optical telescopes supported on a radio dish, and a similar space array. The control system is almost the same in both cases, hence the ground-based array can be considered as a test-bench for the space device. The key points should be demonstrated in a proof-of-concept stage.

Keywords. Optical fibers; telescope arrays; astronomical interferometry.

1. INTRODUCTION

1.1 Optical fibers in interferometric arrays: the idea behind the hardware.

Before the end of the last century, Hertzian-wave optics had been fully explored by Hertz and Righi; all possible configurations of mirrors, lenses and prisms were known to work. When sixty years later radio-astronomical interferometry was born, reference was made to the Michelson stellar-interferometer; nevertheless, optical-type devices were never even considered for handling the beams. Indeed, what had to be handled was not even thought of as a beam, but as a radio signal. Why? Simply because in the meanwhile coaxial lines and waveguides had become commonplace tools. It was felt obvious that the wide-field (in other terms, multi-mode) properties of lenses and mirrors were not required.

When the basic demonstration of interferometry from a pair of optical telescopes was given by Labeyrie (Ref 15), not only was Michelson again treated as the pionneer, but his very tools were reused: photons had to be relayed to the detector by a more complex but not essentially different wave train. Why? Because of an historical accident: the optical equivalent of the single-mode waveguide was not yet available.

Now is the time to stop and think. There is only one essential difference between the radio and optical cases: the numerical value of $h\nu/kT$. For radio sources, the number of photons/mode is practically infinite; for optical ones, it is sadly limited. This affects detection, amplification, heterodyning etc..., not beam properties, nor indeed the need to relay a full beam. If the source can be resolved by the individual telescopes, then there is no point in reconstructing it by interferometry. In any sensible use of a coherent telescope array, the source should be redefined as any fraction of the object which lies hidden within the Airy disk of the individual apertures. Here, opticians can copy radio-astronomers without misgivings.

In other terms, our optical problem is basically a single-mode one, and we should recognize the SM optical fiber for what it is: the natural tool for telescope arrays, wherever applicable, and bring in mirrors as a last resort only. Because of Rayleigh scattering, we cannot hope for improved fibers below 400 nm, which means mirrors will keep one octave of the UV for themselves (actually less from the ground). In the FIR, the lack of transparent materials also seems to mean no fibers in a large part of the space-accessible range.

On the whole, Nature has been kind to interferometrists. Those of the radio breed, for their share, received infinitesimal photons; a happy thought, since hollow waveguides are so lossy as to be worthless without amplifiers. Opticians so far had been unaware of their priceless compensating gift: vanishingly-rare obnoxious phonons. From these, given time, the total-reflexion waveguide was bound to evolve. Let us use it right.

1.2. Actual proposals and demonstrations.

A comprehensive treatment of optical fibers for astronomical interferometry was first given by Froehly (Ref 11). At the 1984 Cargèse ESA Colloquium, we proposed a fiber-linked space array of separate spacecrafts (Ref 5). At the 1987 Oracle NOAO-ESO Workshop, the outline of a much more modest proposal was given (Ref 6) : a

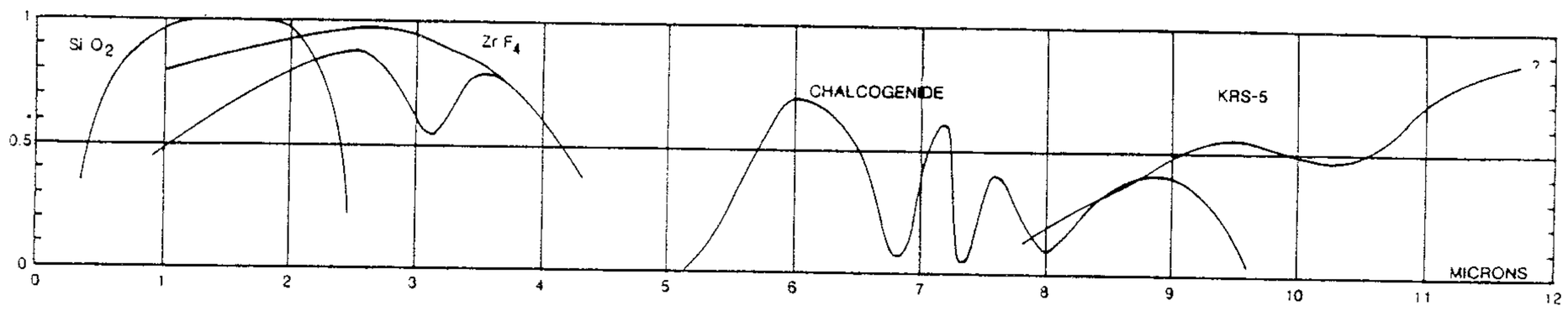

Fig 1. Transmission of various existing fibers for 10 m length. SiO2 (adapted from Ref 5): after many years of intensive work, results are now very close to theory. ZrF4: Upper curve (from Ref 38) is the best laboratory result; lower curve (Ref 17), the first commercial fiber. Chalcogenide (from Ref 39): best result, with a teflon-clad $As_{13}Ge_{25}Se_{27}Te_{35}$ fiber. KRS-5 (from Ref 40), with KRS-6 cladding: curve stops at 11.7 microns because experimenter was mostly interested in CO2 laser beams. Performance appears to be approximately single-mode.

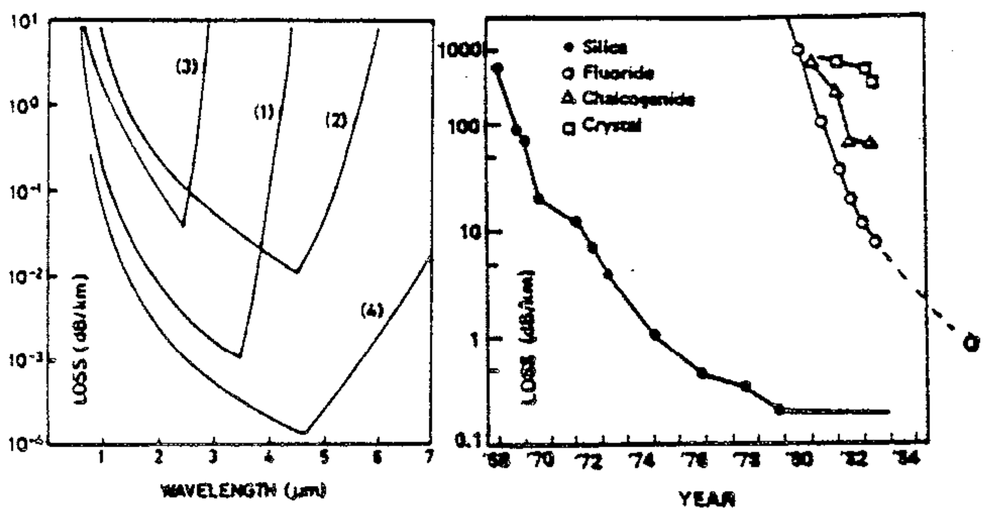

Fig 2. Left, from Miyashita (Ref 19). Calculated losses for 1) halide glass, 2) chalcogenide glass, 3) heavy metal glass, 4) KCl crystal.
Fig 3. Right, from Tran (Ref 36). Reduction of losses as a function of date for fibers of different materials. Point at right added from Ref 38.

radio-dish-mounted array of small optical telescopes; this could be considered a test bench for a generally-similar space array. Both projects will be discussed here in greater detail.

A review of relevant SM fibers properties, together with a discussion of the main advantages and limitations of fiber-linked interferometers compared to all-mirror ones, is found in Ref 5. Additional points were treated in Ref 6, in particular the importance of SM fibers acting as spatial-mode filters for producing accurate visibilities in the presence of guiding and seeing errors. Coupling efficiency into a SM fiber from a perfect Airy disk or from an atmospheric seeing pattern is computed in Ref 22, and our first laboratory demonstration of white light-interferometry through a pair of 30-m SM fibers (in a Mach-Zehnder-type interferometer) is found in Ref 21 . We now have commercial polarization-preserving fibers (Ref 26), and ZrF_4 fibers (Ref 17). Present performance in the visible and IR is shown on Fig 1: while no other fibers have yet matched the SiO2 one, a very-large scale effort is now proceeding in order to make them even better, as theoretically expected (fig 2,3). Lastly, the number of papers dealing with interferometry through SM fibers keeps increasing; a striking development is that of the all-fiber optical gyroscope (Ref 2).

2. GROUND-BASED COHERENT ARRAY ON RADIOTELESCOPE

Rationale for the proposal has been given in Ref 6, and the main points will be briefly summarized. Fig 4 presents the coupling efficiency into a SM fiber through the atmosphere; as one might expect, this is good only for small telescopes. Over the accessible spectral range (400 to 4200 nm so far, with SiO2 plus ZrF4), the Fried parameter r_0 increases by a factor of 17; therefore, the array will be used at IR end of the range on poor seeing nights, and at the visible one on good nights only. Efficient use of larger telescopes means breaking up their pupils into smaller subpupils, and using one SM fiber for each, which by itself is simple and inexpensive. However, this also means having one fast guider per subpupil; furthermore, the already complex fringe detecting system (§ 2.5) becomes even more elaborate. A better (but still more difficult solution) is to use fully adaptative optics, in which case a single fiber is again usable. Altogether, we feel it is preferable to keep the telescopes small and simple and increase their number, because this improves UV coverage, while increasing their size does not. Hence, our proposed array would include many relatively small telescopes (e.g. D=50 cm), each followed by a fast guider, and each connected by a single SM fiber to a central mixing station.

Setting them close to the incident wavefront on a single radio dish (which acts merely as support), appears simpler than scattering them on the ground because a) delay lines are eliminated; b) individual tracking mounts and domes also disappear; c) for each telescope, only the Z position parameter (see fig. 7, 8) has to be taken care of, and the control system is particularly simple. The main drawbacks are an array size fixed by the available radio-dish diameter, and seeing conditions perhaps less than optimum; transporting some dish to a better site is conceivable, but would be a major operation.

Within these limits, we can expect to build a greater number of telescopes for a given cost than in the "ground-hugging" case. Our proposal is intended to produce relatively high-quality but moderate-resolution images; the various proposed ground-hugging arrays (e.g. Ref 16), with much longer baselengths, should be capable of higher resolutions but with coarser coverage of the UV plane.

2.1. General description

The optical telescopes could be located at fixed locations, either around the rim or under the mesh of the radio dish (see fig 2 in Ref 6), hence would not interfere with regular radio operation. Any array shape can be considered. If the dish becomes available full time, one could even have the telescopes radially moving on rails, VLA-like. A radio-dish equatorial-mount should be avoided, because it does not provide field rotation; with an alt-az, base-vectors pivot much as they do in present radio arrays, and image synthesis would be rather similar. The possibly-poor-seeing difficulty has already been stressed; on the other hand, the absence of domes and the high elevation above ground level are favorable factors.

The key is of course the control system, and there are four separate issues. First (§ 2.2) the array must be unaffected by radio-dish errors. The proposed sytem involves a) active guiding on the stellar image; b) passive purely inertial control of Z for filtering out high-frequency vibrations; c) active control of low-frequency Z terms by a system of laser beams used in a geometrical mode (so-called G-control).

Second (§ 2.3), the final path differences at the mixing point are affected by drifts in fiber optical lengths. Passive protection schemes and active interferometric control ("I-control") will be studied.

Third (§2.4) normal-atmosphere dispersion must be compensated. This is independent of fibers.

Fourth, we have the atmospheric-path fluctuations. Overall control of path-difference down to the mixing point is feasible by making use of a fraction of the stellar light, and servoing on the central fringe. Such techniques are fully independent of the use of fibers, and closely connected with basic SNR problems; they will be considered in §2.6, after §2.5 which is devoted to detection techniques. Our philosophy is to to do everything we can to perfect the array *before* fringe-tracking is added.

2.2. Inertial and geometrical control

As just explained, this system compensates merely for radio-dish errors, not for fiber drifts.

2.2.1. Orders of magnitude for relevant terms. We consider three arbitrary points A,B,C, on the radio dish. These define a plane P; guiding errors induce angular variations between P and the waveplane W. We must consider the *linear* guiding errors for each optical telescope, i.e. the locally induced change in distance Z between W and P; moreover, we have dish distorsions relative to P. Any dish will exhibit a lowest resonance frequency N_0 (with $T_0=1/N_0$) due to elasticity of the gears; this will normally be of the order of one or a few Hz. It will be convenient to call flexure all effects at frequencies $N<N_0$, and vibrations all those with $N>N_0$. If the dish has a minimum full-gain radio wavelength λ_{min}, we may rely on having combined guiding-flexure errors of the order of $\lambda_{min}/8$. Vibrations are much smaller, but for that very reason so far remain practically unknown, because they are irrelevant to radio-astronomers.

As a first step, we have measured the linear-motion vibration spectra of two radio-telescopes:

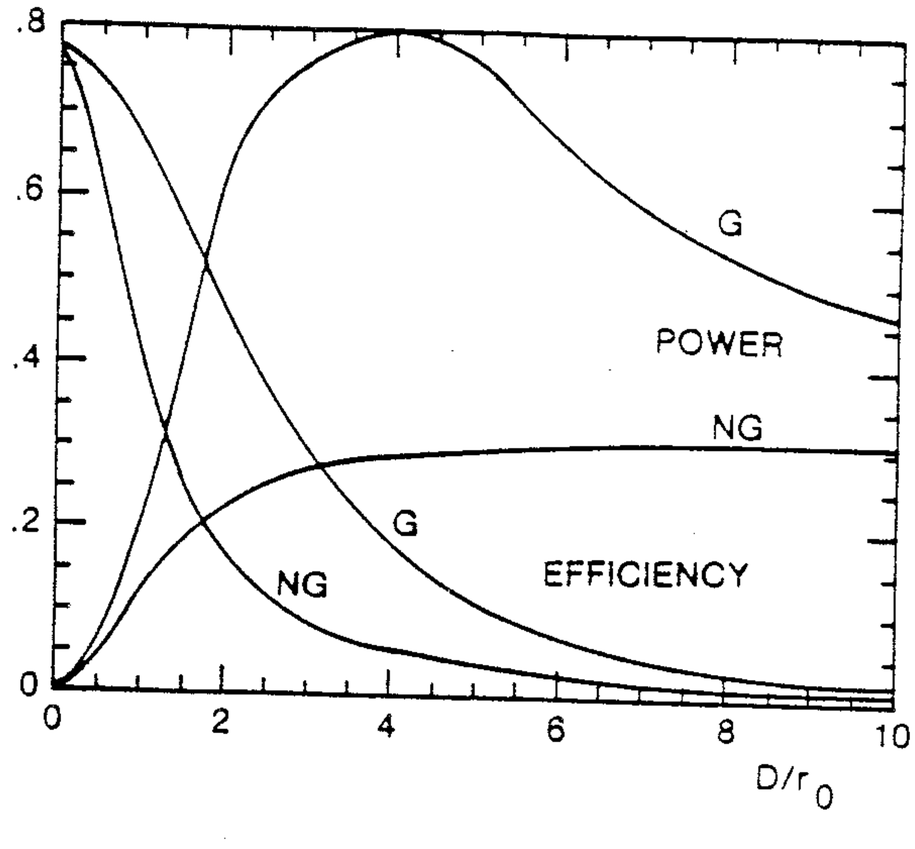

Fig 4. From Roddier & Shaklan (Ref 22). r_0 is Fried's parameter, D the telescope diameter. Efficiency: coupling coefficient C_e into a SM fiber through the atmosphere; scale at left. Power: total coupled power (arbitrary scale). G, NG correspond to the perfectly-guided and unguided cases.

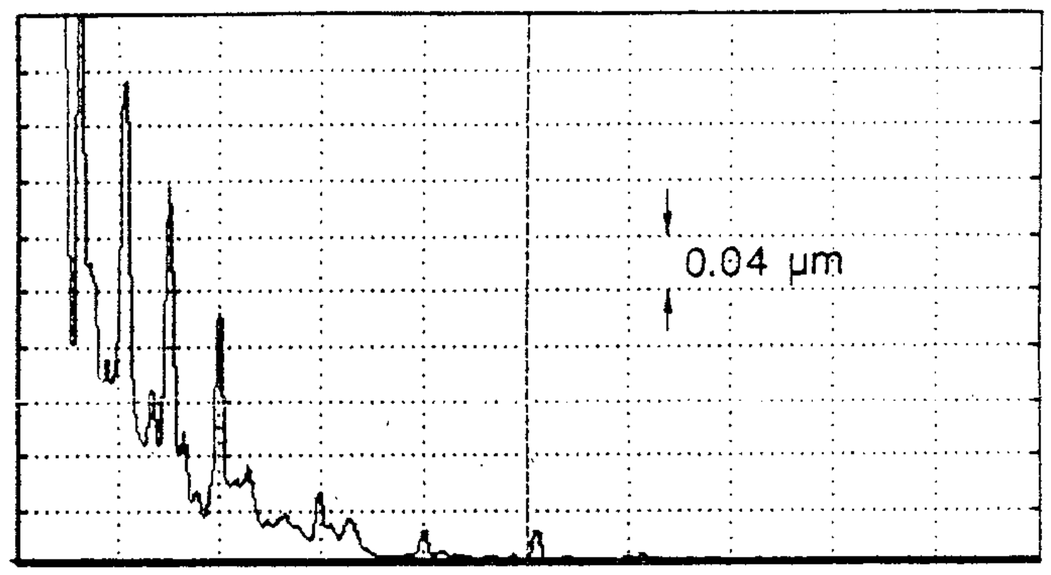

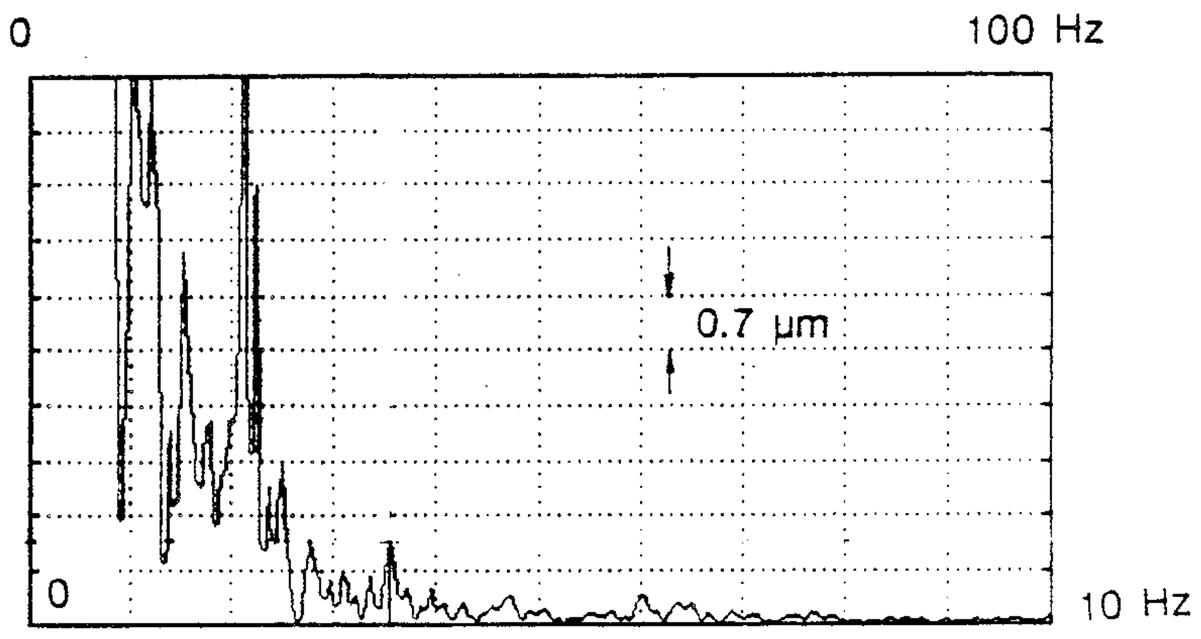

Fig 5. Vibration amplitudes in OZ on rim of Hat-Creek 25-m dish. Endevco Type 7705 accelerometer; minimum detectable accelerations (for a few seconds of integration) of the order of 0.01 cm/s^2 at 100 Hz, increasing by a factor of 5 at 1 Hz. The signal was twice integrated, and a power spectrum plotted with a Type 3561A Hewlett-Packard analyzer. Higher frequency lines are due to drive hydraulic-motors. By hand-shaking the dish, the lowest resonances were identified at 2.1 Hz in OZ, and 2.5 Hz in OY. Here, all low-frequency amplitudes are clearly wind-related; wind velocity was about 12 to 18 Km/h, not sufficiently variable to permit a proper study, and no fast-response anemometer was available. Similar spectra were recorded at Owens Valley, but the double-integration feature was not available. A proper study in the 0.1 to 1 Hz range would be easy with lower-frequency accelerometers.

the Hat-Creek (Berkeley) 25-m, and the Owens-Valley (Caltech) 40-m. As expected, the second (with a λ_{min} of about 1 cm) proved more rigid than the first (λ_{min} about 3 cm). Accelerometer was placed on rim of dish, mostly with the axis pointing along OZ to the star (fig 5), but some tests were also made in the waveplane. We have found the high frequency vibration levels much lower than our naive expectations, which must be attributed to the large size and inertia of the dish: considerably higher amplitudes were found on the pedestal which carries the two axes and the drive motors.

Low-frequency angular errors are well known by radio-astronomers. High-frequency ones again are not; we have not attempted a direct measurement (this requires two accelerometers), but one predicts (from fig 5 and some sensible assumptions) that they will be smaller than the atmospheric terms, and the fast guiding problem not different from that for a ground-hugging array. In order to get close to the "guided" curve of Fig 4, guiding should be somewhat smaller than the seeing disk diameter (e.g., below 1 arc sec), and response time short enough to freeze the phenomenon (e.g. 10 ms in the visible, increasing in the IR). The guider we have described in Ref 4 is suitable; with the much smaller mirrors required here, response time would be about 3 ms. Of course, performance will degrade for faint objects (see §2.2.2.).

We now consider path differences. Insofar as feasible, we want to operate our coherent array as a so-called absolute one, or, in other terms, in a "blind" mode. Then, the rule is that residual internal errors should be smaller than those induced by the atmosphere; still, there is no point in making them *very much* smaller, astrometry not being a goal. Orders of magnitude can be derived from the Fig. 6 computed curve, which gives the absolute effect. A more refined analysis should start from the measured differential ones (Ref 18,29,34). Conclusion is that errors of several microns will be tolerable in the VLF range, but these must decrease at higher frequencies.

2.2.2. Control system description. While astro nomers have ultimately consented to run their world-machine along Copernican-Galilean guidelines, they are still observing it through telescopes cranked with orthodox Aristotelian-Ptolemaic tools. Today, the standard blueprint remains: A telescope is a moving device (which is pure Ptolemy), and it may be kept on the move solely through our ceaseless exertions (sheer Aristotle). While in space this attitude is immediately perceived as inadequate, it nevertheless has been the only practical one on the ground. For our telescope array, a Newtonian-type approach: *Leave well alone*, becomes not only more natural but hopefully simpler, both on the ground and in space.

For time intervals shorter than a certain time T_c, the array is inertially suspended: it floats over the radio dish, whose sole function is to support the weight, not to define shape nor orientation in any way. T_c is the *intrinsic coherence time* of the array: it is the time during which our system remains fully coherent without any help from astronomical photons. Next, we must apply *slow* corrections (i.e. with a response time greater than T_c), which are needed for three main reasons: a) No inertial

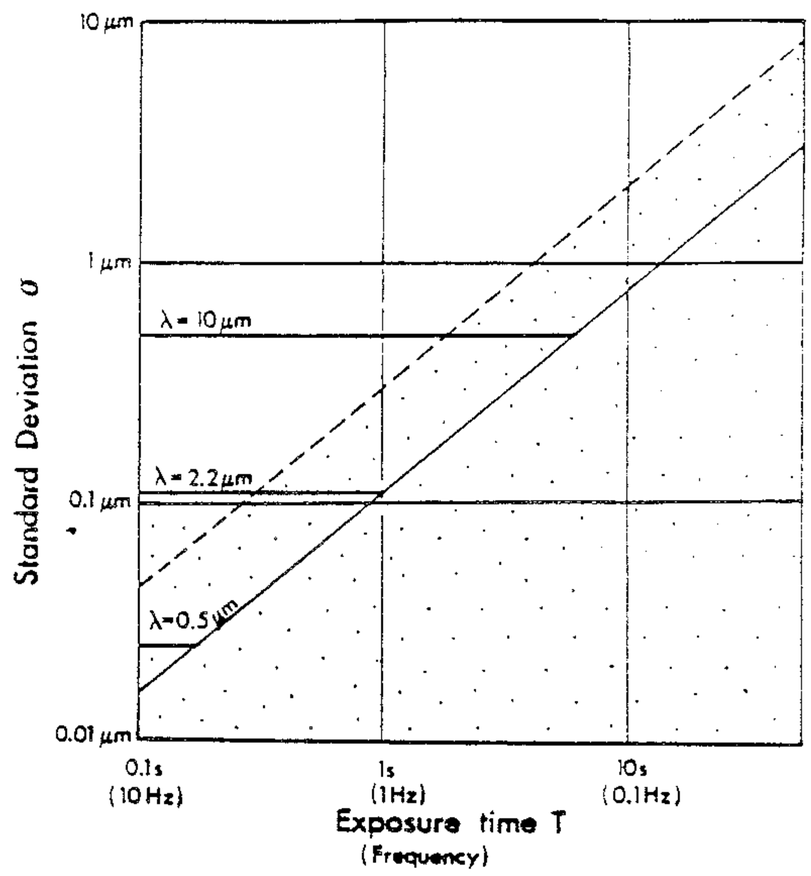

Fig 6. From Roddier in Ref 24. Computed RMS path length fluctuations through the atmosphere for time T. Full-line: "lucky-observer" model; dashed: standard conditions.

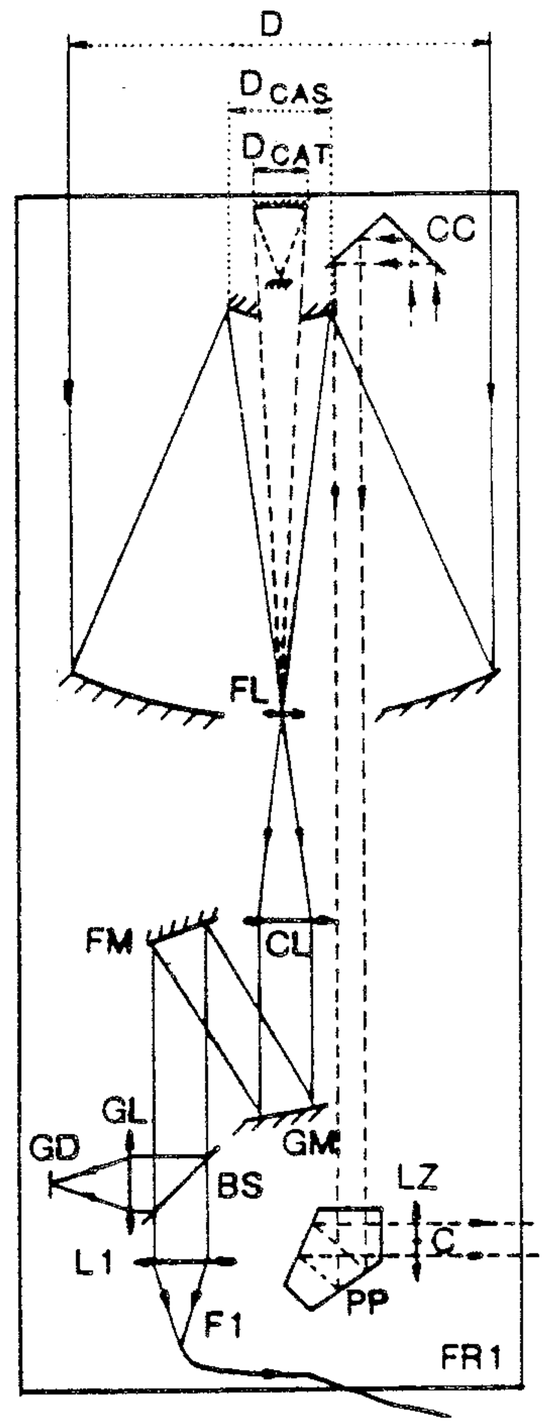

Fig 7. Optical system (master-telescope case). Full lines represent the astronomical-beam path. The G-control laser beam first follows the same path, but in the reverse direction; a small fraction (dashed lines) is returned downwards. FL, CL: field- and collimating- lenses; GM, FM: guiding- and fixed- mirrors; BS: beamsplitter; GD and GL: guiding detector and associated lens. F1, L1: fiber input and associated lens. CC, PP: cube-corner and penta-prism. LZ (with optical center C) focuses the laser beam on DA,DB of Fig 3. Cat's eye in the center of the Cassegrain returns some laser light into the fiber (see § 2.3.2).

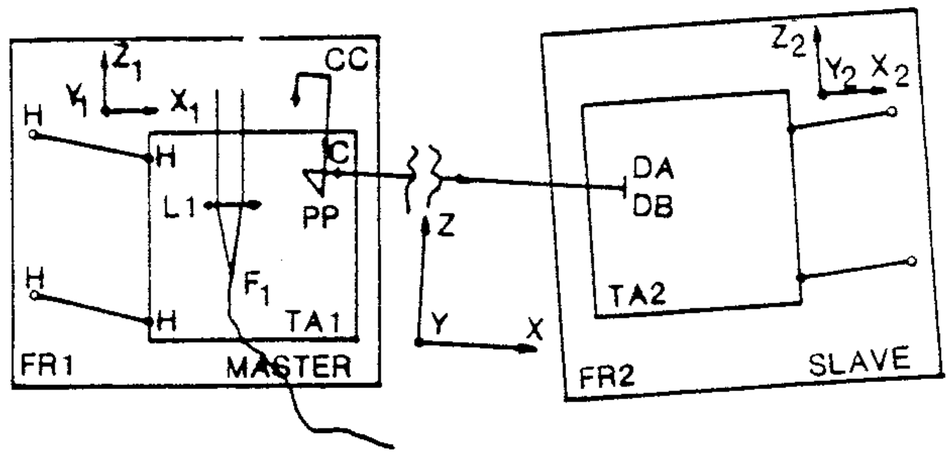

Fig 8. Inertial-geometrical control system. Optics of telescopes and guiders, actuators and sensors not represented. H: flexure-hinges. OXYZ is star-oriented; $OX_1 Y_1 Z_1$, $OX_2 Y_2 Z_2$ are linked to FR1, FR2. Laser system detects motions in OZ of C relative to detectors DA, DB irrespective of other motions, which are uncontroled.

suspension being perfect, small residual forces do induce slow drifts of the array relative to inertial space; b) light aberration makes the star as-seen-from-Earth move in inertial space; c) normal atmospheric refraction induces a second small shift. The required error signal is given by a laser beam system which accomplishes two goals: it rigidifies the array by connecting all "slave" telescopes to one "master"; second, it keeps the whole array pointing to the time-averaged atmosphere-refracted star image. The first is easier than the second.

The core of the system is shown on Fig 7,8. Both master and slave are carried by identical frames FR1, FR2, attached to the dish. Each telescope is aplanatic, and followed by its own guider; telescope-plus-guider form an afocal system, and the output is a collimated beam with a diameter of the order of 1 cm. Pupil is imaged on the fast-guiding mirror, which produces a stabilized stellar image on its own two-dimensional position-sensing detector, and by way of consequence, on the fiber input. We have corrected the angular errors (both from the atmosphere and the radio dish) in a perfectly standard way.

We now have to keep the path-difference constant (initial nulling is performed in front of a collimator). Transverse motions of FR1, FR2, in OX, OY are irrelevant: this is one fundamental advantage of a waveplane-mounted fiber-connected array. Furthermore, motions in OZ of telescope-plus-guider do not alter path difference either (but internal rigidity of the afocal system is essential). Altogether, path difference is solely affected by motions in OZ of the small tables T_{A1}, T_{A2}, which carry only the condensing lenses and the fiber inputs. These are supported by parallelogram-type suspensions with standard flexure-hinges (Bendix-type); maximum displacement (fixed by radio-dish errors) could easily be a few cm. Essentially, we want to keep T_{A1} and T_{A2} at constant distances from the wave plane.

Fast and slow errors are corrected in two different ways. The first will be filtered-out by table inertia: the supension may have an arbitrarily low resonant frequency (far below N_0), and very low damping, due to an active feedback scheme from position and velocity transducers; these permit compensation of the elastic and damping forces respectively; correcting forces are applied by loudspeaker-type actuators. All of which forms a high-attenuation anti-vibration mount, similar to those used for supporting GW detectors (Ref 27). Table mass is limited by the maximum weight component in -OZ which the actuators can carry, and ultimate performance mostly by elastic-torque drift and/or residual solid friction within the hinges. Linear air-bearings offer another possibility, with different limitations, but are not applicable in space.

The slow errors are compensated by an active system in which the force is produced by the same actuators, and the Z shift measured by a laser beam coming from the master table T_{A1}, and falling on a one-dimensional position-sensing detector carried by the slave table T_{A2}. The error signal is sampled at frequency $N=1/T_c$; this is adequate for correcting all errors at frequencies lower than N/2. Plenty of laser energy is available, hence our sampling time T_s (during which the laser-beam is on) may be a small fraction of T_c; for instance we might have T_c=1s and take T_s=0.1s. The astronomical beam is not used during T_s, and there is no stray-light problem.

Geometry of the laser beam is now described. Let OZ be the time-averaged direction of the star, OXY that of the waveplane. We consider the master telescope. Because the guiding detector GD and lens GL are supported by FR1, the collimated-beam direction is fixed within FR1; let us call it OZ_1. The (OZ, OZ_1) angle is a function of flexure, tracking, and initial alignment errors; system could tolerate anything up to roughly 10 arc min. The laser beam is fed from the mixing station through the fiber; it passes through the guider, illuminates the full master-telescope pupil and emerges as an upward-travelling collimated beam. While the laser is switched on (during T_s), the fast-guiding mirror is frozen to its *time-averaged position* over the previous cycle of duration T_c. Hence, our outgoing laser beam is parallel to OZ irrespective of all mechanical tilts.

A fraction of the energy is intercepted by a cube-corner prism CC and returned along -OZ down to T_{A1}. The beam is next deflected by pentaprism PP at a right angle; it is now parallel to the waveplane. Several different detection schemes are possible; in the simplest (shown on Fig 7,8), a lens Lz on T_{A1} focuses the beam on a detector pair carried by T_{A2}, and relative shifts along OZ between T_{A1}, T_{A2}, are detected. With D=50-cm telescopes, a d=3cm beam, an L=20m master-slave distance, a P=1 mw laser, 0.1 transmission and room-temperature Si detectors (NEP=7 10^{-14} $w/Hz^{1/2}$), we find a RMS error of about 0.3 micron in T_s=0.1 s.

The narrow laser beams could be put in vacuum pipes, but this is probably not needed, because the air-induced fluctuations should be small compared to the whole-atmosphere ones of fig 6, which the system is *not* intended to correct anyway. The requirement of internal rigidity for the telescopes appears more difficult at first glance. However, these telescopes are small, hence their internal resonances will be relatively high (roughly, above 10 Hz), and they can be tuned so as to avoid the excitation frequencies, such as those of Fig 5. Moreover, since the supporting frames FR1 etc... do not need to be accurately pointed, they can be attached to the dish by standard antivibration rubber pads, which provide fair attenuation in that range.

The second limitation comes from the guiding. It is reasonable to make the master-telescope somewhat larger than the slaves. We take for instance D=1m, 0.1 transmission, a 400-700 nm range, a GaAs guiding PM with mean QE=0.1, and a

1 arc sec seeing disk. The guiding signal is integrated during time T_c; supposing e.g. T_c=1s, we find a RMS guiding error of 3 m arc sec on a magnitude-8.5 star; the corresponding RMS *dZ* becomes equal to that of Fig 6 ("average" case) for a 20 m master-slave distance, i.e. a 40 m maximum-baseline array. Whether actual guider performance can reach this level remains to be seen; in any case we cannot hope to "blind-track" the array-fringes on fainter objects, and actual fringe-tracking must definitely be added if feasible.

The fast-guiding performance of the same system must also be given: again with a 1 arc sec seeing, it is reasonable to ask for (very roughly) guiding within 0.3 arc sec in 10 ms in order not to degrade too much the Fig 4 "guided" curve; this requires 1000 times less photons, and will be feasible on a magnitude 16 star: the limitation is much less severe.

One should stress that all this G-control is far simpler than any system required in a ground-hugging array, with or without fibers, in which case all telescope parameters (linear and angular) must be fed-in if one tries to operate the delay lines in a "blind" mode. The essential difference is that telescopes are now close to the waveplane, and the same will be true in space. The various servo loops and mechanisms are similar to those already used in a family of Fourier spectrometers (Ref 4,8), but simpler, since the desired accuracy and bandwidth are both much lower. A detailed study (optical system, adjustments etc...) will be given elsewhere.

2.3. Control of fiber optical length.

Long fibers on a radio dish will exhibit variable path lengths because of differential temperature and gravity effects. The problem is conceptually similar to the one astronomers have long battled against in their telescopes, but much simpler: any large mirror is an optically multi-mode and mechanically multi-parameter device; moreover, it cannot be enclosed. For fibers, simple non-optical schemes should be tried first; the ultimate refinement is active interferometric control.

2.3.1. Passive non-optical control. First, we tackle temperature effects. Path-length temperature coefficient for a fused silica fiber is of the order of $10^{-5}/°$ (see Ref 5). With a 40-m dish, the maximum fiber length (at least along their separated paths) is 20 m, and a 1/100° temperature difference will induce a 2 microns path-difference; this is comparable to what we get from the atmosphere at 0.1 Hz (fig 6). The brute-force approach (which may even work) is to enclose the fibers in double walled pipes, and circulate a fluid (eventually, a coolant). A subtler, but compatible, solution: if the fiber and a resistive wire are stretched close to each other and kept at the same temperature (e.g. within a copper pipe), the optical length and resistance will show the same time-variations, even if the temperature is not uniform along the length. Then, active temperature control of a small fraction of the total length, using the resistance change as error signal, provides a simple correction.

Second, the fibers (having different orientations on the dish) will stretch differently under variable gravity. If response was linear (purely elastic distorsions), a smoothly varying and repeatable path change would appear, the correction of which is elementary. However, one may fear that solid friction between fiber and support will induce unpredictable jerks. Perfect solution is immersing the fiber (perhaps enclosed in a flexible sleeve) within an equal-density fluid. We are left with variable hydrostatic pressure, which will be smooth and predictable. More convenient all-solid solutions will perhaps be found, much as for mirrors.

One may hope that such techniques will prove adequate in the ground-based case. However, in space we shall propose a fully-phased array: all path errors must be small compared to the wavelength. Then, active interferometric control of the fibers becomes unavoidable, and this should be tested first on our radio-dish array; hence, the discussion is given here.

2.3.2. Active interferometric "I-control". Whenever long separated interferometer paths have to be used and the highest stability is required, interferometric control must be applied, and such systems have been proposed for all-mirror arrays. A fiber interferometer is not different in this respect, but in practice the problem is simpler: again there is only one parameter to control, fiber optical length, while any system involving several mirrors has many degrees of freedom. Situation with fibers is close to that of radio-arrays where waveguide delay is controled by propagation of a local oscillator signal (see e.g. Ref 35).

Similarly, a laser signal may be fed into all fibers from the mixing station, reflected at the telescope ends, and returned to the origin. Residuals to be corrected should be mostly drifts, hence again the error-detection can be discontinuous, and the laser is switched on and off. Since fiber lengths are almost equal, a high-stability laser is not needed, and the same one can be used for both the I- and G-controls. We have a choice of active elements: wedge-compensators, or heating-up a fiber section as demonstrated in Ref 9 (indeed, for phase-locking an interferometer).

There are two optional interferometric configurations. First, the fibers could be turned into Fabry-Perot etalons by putting semi-reflecting coatings on the input-output ends, as demonstrated in Ref 30 with finesses up to 500. Here, low finesse is adequate, which means low reflectivities and small loss of astronomical photons; also the laser wavelength may be outside the astronomical band. This approach checks solely the fibers, not the residual air paths. Preferably, any pair of fibers may be incorporated into the arms of a Michelson-type interferometer; laser, beam-splitter and detector are located in the mixing station, and small retroreflectors (e.g. cat's eyes) in the center of the Cassegrain mirrors (fig 7). Let D_{cas} and D_{cat} be the Cassegrain- and cat's eye diameters respectively. Telescope obstruction ratio is $K=D/D_{cas}$; this is not worsened if we take $D_{cas}/D_{cat}=K$; then, the fraction of the laser energy coupled-back into the fiber is K^{-4}. For instance we select D=50cm, K=4, D_{cas}=12.5 cm, D_{cat}=3.1 cm; with the same laser, transmission factor, and detector-type as above, and again within T_s=0.1s, the computed RMS path-difference error given by the interferometer is less than 0.1 nm (and far less than in the G-control). Stray light reflected by various elements (e.g. fiber ends) must be discriminated against, by putting

the small mirror of the cat's eye on a PZT driver (exactly as done in FTS, Ref 4); each telescope would be identified by a different frequency. Lastly, if we use two laser wavelengths, we are able to reconstruct two separate error signals, one for the fibers and one for the air paths.

2.4. Compensation of atmospheric dispersion.

Normal-atmosphere dispersion has two main consequences. First, the stellar images are spread out as small spectra. A given fiber will never be used over more than one octave, and the worst-case would occur over the 400-800 nm range. At 45° elevation we get 1.5 arc sec dispersion, which is comparable with the seeing-disk under good conditions; hence, at both end of the range, the seeing disk becomes off-centered on the fiber input and energy loss occurs. Compensation by introducing some chromatic aberration is simple, but perhaps not worth the trouble, since the use of this whole particular range may be exceptional.

Second, the air paths to the telescopes are different; the problem can be rigorously solved only with long vacuum delay lines, which we reject. Fortunately, the dispersion curve of air within our accessible range is similar to that of common IR-transmitting crystals. Worst-case would again be in the visible. We find that with a 40-m radio dish pointing at 45° elevation, the extra air-path is 40 m, which gives 280 microns of path-length change between 400 and 800 nm. Compensation would require e.g. 6.7 mm of KBr; peak-to-peak residuals in the range are +/- 4 microns, which is comparable to the VLF errors in Fig 3. These residuals become much smaller if the range is reduced, or in the NIR; as stressed in §2.5 and 2.6, image reconstruction is unavoidably performed within narrow spectral slices. In order to accomodate changing elevation, wedge-type compensators are required; atmospheric dispersion being fully predictable, these will be programmed, not servoed, and the required displacement accuracy is moderate. A compensation of this type (using piles of glass plates) has been demonstrated by Koechlin in the CERGA interferometer (Ref 14).

2.5.Astronomical-fringes detection schemes.

We now consider the detection of the astronomical signal. This is a complex problem: in the spectral range already open to fibers, one goes from almost pure photon noise at the visible end to predominant detector noise in the NIR, and one already reaches the thermal noise region. We shall have to use not only different detectors but also totally different detection schemes. Here we merely outline two possible solutions, denoted spatial and temporal multiplexing; neither has been fully worked out.

Two preliminary remarks: First, starting from our N telescopes, simultaneous detection of fringes from all M=N(N-1)/2 telescope pairs is desirable. We have to do it from a given number of photons, which must be split into separate paths. This is independent of fibers.

Second, fringe visibility is a function of the ratio of baselength over wavelength: the spectral range must be small for accurate image reconstruction. Hence, our overall range must be broken into narrow slices, and the reconstruction process carried out separately in each. In the pure photon noise case, we can in principle use arbitrarily narrow slices: if the object is achromatic, results can then be averaged, and ultimate SNR is not affected. If detector noise is the limit, and if we have to increase the number of pixels to observe our slices, then SNR degrades. In principle, this loss could be avoided by using Fourier spectroscopy, as shown by Ridgway (Ref 37) from two small apertures within one pupil. We have suggested a solution (Ref 5) for the two-telescope case, but we have not found one for a many-telescope array, hence dispersion seems to remain necessary. The choice of slice width will result from a compromise between noise errors

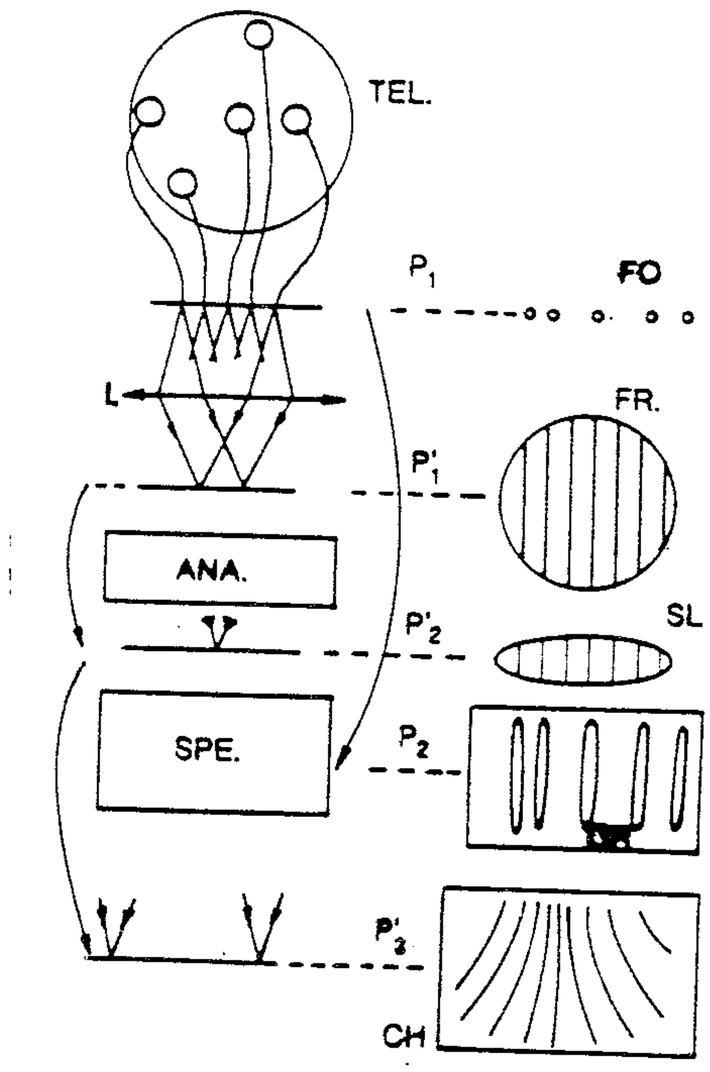

Fig 9. Spatial multiplexing. Fiber outputs FO are aligned, with non-redundant spacings, along OX in front focal-plane of lens L. The diverging beams superimpose in the back focal plane where the fringe patterns FR are formed. A standard anamorphoser ANA (not an image slicer) squeezes these patterns along the spectrograph SPE input slit SL, and simultaneously spreads the fiber-outputs images over the grating (or prism) GR. Finally, a two-dimensional channelled spectrum CH is produced at spectrograph output on the detector. Conjugation of successive planes is shown.

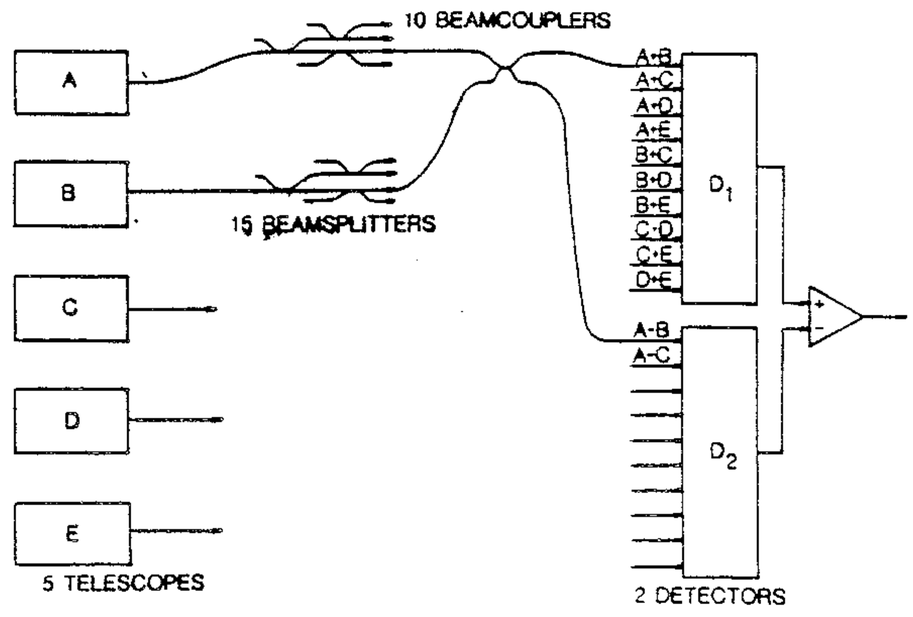

Fig 10. Temporal multiplexing: schematic fiber-optics system shown for 5-telescopes case.

and systematic errors; these last increase with slice width. Again, this has nothing to do with fibers.

2.5.1. Spatial multiplexing. This has been proposed (Ref 6A) for the photon-noise range, in which it is permitted (and presently feasible) to use large number of pixels. The scheme is merely an adaptation of that originally described by Greenaway (Ref 12), but fibers make things much easier. We start from N telescopes forming a two-dimensional arrray (fig 9). The N fiber outputs are aligned so as to form a one-dimensional non-redundant array. A two- dimensional many-pixels detector observes the interference pattern at infinity; each fiber pair produces a different spatial frequency, which can be separated in the final analysis. A grating or prism provides dispersion perpendicular to the figure plane, hence separate measurements are made within each slice.

2.5.2. Temporal multiplexing. In the detector noise domain, we want to reduce pixel numbers. The proposed scheme (Ref 6A) measures all M interference signals with just one pair of pixels per spectral slice; dispersion (and more pixel pairs) is still required to cover any wide spectral range.

The optical system may eventually contain only fibers (fig 10), although this is not essential. First, we transfer the light from telescope to mixing-station MX through N long fibers; next, each is subdivided into N-1 daughter ones, in order to mix it with similar daughters coming from the N-1 other telescopes. This is done with standard X-couplers, here operating as mode splitters, i.e. as one-input two-outputs devices: one of the regular inputs is left unused. These are now commercial (Ref 26), but so far their bandwidth is too small. Next, we need M other X-couplers operating as mode mixers; the two inputs and two outputs are needed. We must equalize separately all the telescope-to-splitter paths on the one hand, and all the splitter-to-mixer paths on the other; fine adjustment will again involve temperature-control. After the mixers, we are out of the interferometric paths: fibers no longer have to be equal and stable. Each detector sees the outputs of M fibers in parallel; all fiber ends are aligned in the figure plane. A prism or grating again introduces dispersion, and each of the two illustrated detectors is only one pixel within a one-dimensional array.

Finding a suitable modulation technique is a separate problem (it could be applied to an all-mirror array), and one not fully solved so far. In a perfect scheme, N caracteristic time-modulation patterns would be applied at each of the N telescope outputs and M fully separable patterns seen by the two detectors. A bandwidth of the order of 100 Hz must be allocated to each reconstructed fringe signal, in order to sample correctly atmospheric phase shifts. First, efficiency must be high, which implies pure phase modulation; situation is comparable to that of so-called internal-modulation Fourier spectroscopy (Ref 3), in which case about 75% efficiency was realized over a one-octave spectral range with a $\lambda_m/4$ amplitude sine-wave modulation (λ_m being mean wavelength). This can be achieved here by mounting a small mirror on a PZT driver (as in FTS), or by wrapping a length of fiber on a PZT drum (now common practice). Also, photoelastic modulators provide half-wave modulation at up to 80 KHz throughout the fiber-accessible range (Ref 13), while InSb detectors are usable up to roughly 100 KHz.

Second, there must be sufficiently low cross-coupling between the M output signals, and this is more difficult. Here is a simple-minded attempt: to telescopes A, B, C...we apply N "carrier" sine-waves with equal amplitudes $\lambda_m/4$, and frequencies F_a, F_b...F_n. The time-variation of path-difference for the A,B pair is

$X = \lambda_m/4 * (\cos(2\pi F_a t) + \cos(2\pi F_b t))$ and the fringe signal will contain all "sidebands" with frequencies $pF_a + qF_b$ (p,q, integers). Efficiency comparable to that in FTS is realized by using only all the pairs of first-order sidebands $F_a + F_b$, $F_a - F_b$ ... . We have easily found, by trial-and-error, carrier sets for which these first-order sidebands are sufficiently well separated. For instance, in one solution for N=9, M=36, preserving 100 Hz bandwidth, the highest carrier is at 11.1 KHz, and the highest sideband is at 20.2 KHz. Unfortunately, the unused higher-order sidebands (p,q>1) have non-negligible amplitudes, and some of them fall close to some of the used ones. Since there is still plenty of bandwidth to spare, better solutions should exist, but they will require a computerized search. Perfect separation of all M channels is probably impossible, but residual leakage will be stable and fully computable; a CLEAN-like process may be applied a posteriori.

2.6. Astronomical-fringe tracking and signal to noise ratio

We start from the general discussion of SNR in ground-based, long base-line interferometry given by Lena & Roddier in Ref 23. An important result is the slow increase of the SNR as the telescope diameter D increases beyond the scale r_0 of atmospheric fluctuations, unless real-time compensation of these fluctuations is made. For this reason, Shao & Staelin at Mt Wilson, and Davis & Tango in Sydney, have built interferometers with small apertures. In this case, SM fibers have good efficiency (see Fig 4), and the same expressions hold for the SNR whether fibers are used or not. In Ref 23 is found the limiting magnitude with photoelectric stellar-fringe tracking, either in the visible or the IR: an error signal is obtained from the white-light fringes, and used in a servo-loop to operate actuators that compensate for the random atmospheric phase-delay. Main conclusion is that passive fringe recording (without tracking) provides higher sensitivity only if one has absolute pointing capability, and that even so the gain remains small in the visible, and there is no gain in the IR. Reason is that fringe tracking can be done with very large optical bandwidths, whereas passive recording requires bandwidths narrow enough for the light to remain coherent despite the path fluctuations. For instance, in Ref 29 Shao was able to track fringes on Polaris with 1.27 cm apertures and 500 nm bandwidth (GaAs photomultipliers), while Davis in Ref 7 used 48 min of integration time T_i to determine the diameter of Sirius with 10.6 cm apertures and 0.3 nm bandwidth.

In the visible, where photon noise dominates, the light can be spread out over multiple spectral channels. The SNR from passive recording keeps increasing as $T_i^{1/2}$, bringing back some gain at the expense of complex data processing. This is

the approach taken by Labeyrie at CERGA. However, as soon as more than two telescopes are used, SNR decreases as an inverse power of the number of telescopes coupled together, and data-processing becomes even more problematic. In the IR, the passive-recording SNR increases only as $T_i^{1/4}$, and no gain is obtained under realistic conditions. Moreover, when detector noise dominates, spreading the light over too many spectral channels ruins the SNR. On the other hand, if the § 2.5.2 scheme can be developed, the SNR does not depend on the number of telescopes, and the operating mode is a close analog to that of a radiointerferometer.

As a result of the above discussion, we plan to track fringes over the maximum allowable bandwidth. Different fibers will be used for different spectral windows; for each window, bandwidth will be limited either by the fiber to about $\Delta\lambda/\lambda$ = 0.5, or by the width of the window. In the red or the IR, the wavefront distorsions are nearly achromatic (Ref 25); it is therefore conceivable to use all the light from e.g. 0.5 to 5 microns to track the fringes and cophase an array of telescopes, provided all instrumental path-differences are controled with enough accuracy (e.g. as proposed in §2.2 and 2.3). Here we shall give limiting magnitudes for fringe-tracking either in the visible or in the 2.2 microns K-band, using results of Ref 23. We take the same conservative value of r_0 = 10 cm in the visible (1 arc sec seeing), and use the same values for atmospheric stability time t. First, in the IR: we take D=60 cm, which means D/r_0 = 1 at 2.2 micron, and we consider the "guided" case, for which fig 4 gives C_e=0.65. We assume 0.1 overall transmission, and a detector with QE=0.7 and NEP = 10^{-16} W/Hz $^{1/2}$. With the bandwidth of the K band, a magnitude-7.5 star gives SNR=5 on the fringe amplitude, or +/- 12° on the phase. Next, in the visible we assume D=40 cm (i.e. maximum power on Fig 4), which gives C_e=0.18. We take $\Delta\lambda$=300 nm, QE=0.2, and we get a SNR of 5 on a magnitude-9.8 star.

Phase closure relations are taken into account to disentangle atmospheric phase errors from the object-induced phases. Since (in the visible), the SNR decreases when photons are shared over many baselines, we will track the fringes only over the smallest baselines associated with each telescope. These baselines provide the highest fringe visibility, hence the highest SNR; this procedure is a close analog of an adaptative optics system using a shearing interferometer as wavefront sensor.

Whereas fringe tracking will be done using the widest possible bandwidth, image reconstruction requires much narrower ones. An obvious limitation is the wavelength dependence of the spatial frequency with a given baseline; another may be the wavelength dependence of the object structure. Dichroic filters will be used to separate image-reconstruction light from fringe-tracking light, and different detectors used as in an adaptative-optics system. Since fringe tracking corrects in real time atmospheric-path fluctuations, a large T_i can be used in image reconstruction. This will provide extreme sensitivity for narrow-band work such as imaging stellar chromospheres in H light, or other applications.

The general conclusion is that basic SNR problems are little affected by the use of fibers, and most of this discussion could have been given in a different context. No attempt is made here at predicting SNR in the final reconstructed images; this should be done mostly by numerical simulation.

3. SPACE-BORNE PHASED ARRAY

3.1 General considerations

SM-fiber links can be incorporated into the design of any of the proposed connected-elements space interferometers, just as it could be done for TRIO-type free-flyers (Ref 5). The basic advantage remains a considerable relaxation of positioning tolerances, and the control systems just discussed remain directly applicable. Actual shape of the array is irrelevant: We might try a linear, or O- or Y-shaped array. Common feature is that in all cases, the telescopes are close to the waveplane, just as on the radio dish. Since the supporting framework will be not only flimsy but also crudely guided, the array can be made much larger than if we were trying to hold together an all-mirror system. Distorsions dZ of the order of 10 cm would be allowed; it should prove feasible to combine inflatable structures (as presently studied by ESA) with standard thrusters and/or reaction-wheels.

As an example, let us explore a solution which makes use of an already well-advanced project. The Large Deployable Reflector will be a 20-m telescope, designed for the FIR and diffraction limited at 30 microns (Ref 33,20). We propose to add a set of small telescopes, very much as on our radio dish. These would be placed mostly around the rim, but some could be added behind holes in the FIR panels, because of the limitations of a pure-ring array. Unlike on the ground, moving the telescopes would be impossible, but full azimutal scanning is available by spinning. Observations could be simultaneous with the FIR ones. The cost to the original program includes a) added weight, which obviously limits the telescope diameters, even if the atmosphere no longer does; b) holes in the panels cause a small loss of energy and perturbation of the diffraction pattern in the FIR; c) thermal radiation from our optical telescopes may have to be blocked off; d) the LDR must be able to spin.

A general discussion of SNR is provided by Roddier in his review on "Imaging strategies for a space borne interferometer"; it will not be repeated here. The case for fibers is much simpler than on the ground, since one immediately finds that the C_e into an SM fiber from a perfect Airy pattern is about 0.8. The conclusion is again that basic SNR is hardly affected by the use of fibers.

3.2. Control systems

A discussion of fringe-tracking (from the astronomical source) would differ little from the ground-based one, and is independent of fibers anyway; hence none will be given here. We concentrate on the techniques required for stabilizing the array *before* fringe-tracking is applied. Our G-and I-controls are unchanged in principle. Still, there is one capital difference: since we have no atmosphere, we try to build a *phased* array, and all residual errors must now be a small fraction of the wavelength, a far more stringent requirement. Internal and external problems will be considered separately.

3.2.1. Internal problems (G-and I-controls). The I-control is unchanged compared to §2.3.2, and sensitivity is fully adequate. However, improved performances of the inertial and geometrical controls is required; both look feasible.

First, the attenuation provided by the inertial suspensions will be far greater, because stray forces from the hinges (which no longer have to carry weight in OX, OY) become smaller, and T_c is much increased. Furthermore, it is possible to put on each of the small tables T_{A1} etc.... a free-floating-ball accelerometer whose output is fed to the actuator, so that table acceleration is nulled. Our tables then operate as small drag-free satellites (in OZ only). At this point, the distinction between a connected-elements array and one made of separate free-flyers, begins to blur: the framework functions merely as a convenient way of getting the telescopes in station. Also, it may be used as a momentum sink, for applying forces to counter known gravity gradients, making the solution applicable to a low-orbit. Much weaker unknown residual gradients from the Earth will remain a limitating factor, while those from the spacecraft itself would probably set the limit to the acceptable framework distorsions.

Let us call g_m the minimum detectable acceleration, dZ the tolerable drift in Z; we may now take $T_c=(2\ dZ/g_m)^{1/2}$, i.e. the time needed for the array to drift by dZ. T_c is still the intrinsic inertial coherence-time of the array, i.e. that during which no G-control laser photons are needed to keep the array rigid, and (more important), no astronomical photons to keep it guiding on the source. Free-ball accelerometers in space experiments (DISCOS aboard TRIAD, Ref 32; CACTUS aboard CASTOR, Ref 1) have exhibited stray accelerations of at most 10^{-6} cm/s^2; taking this as g_m, and putting dZ=0.5 micron, we find T_c=10s. However, the acceleration residuals can be modeled, and further increases of T_c seem possible.

Second, sensitivity of laser-beam detection in OZ must be improved. Keeping all the same parameters used in § 2.2.2, but substituting Ga-As photomultipliers with QE=0.1 to the Si cells, we find that RMS error in OZ is reduced 100 times, down to 3 nm; since we have just shown that T_s could be much increased compared to the 0.1 s figure we used on the ground, it is clear that sensitivity is more than adequate. However, in order to eliminate DC drift, the simple two-detector scheme must be replaced by one using modulation and a single detector. Actual accuracy is harder to predict: angular stability of small prisms is known to be very high, provided adequate shielding against temperature gradients is used; still, our laser beams are all reflected by the central portion of the master-telescope mirror, hence they merely transfer to the whole array whatever stability this mirror exhibits. Best performance will be achieved if it is made of Zerodur-type materials, and kept at the zero-expansion point.

Essentially the same G-control could be applied to a free-flyers array, with a much longer distance L. RMS error in OZ is proportional to L, and to d^{-2}, but one cannot increase much the size of the prisms. Still, sensitivity can be improved by spreading or splitting the beam in OZ at the output of T_{A1}. In one possible solution, the optical diagram remains the same, and much larger prisms CC and PP are simulated by small mirrors held in place by optically-contacted spacers. Again, the true limitation will be stability of these devices.

3.2.2. External problems. Even if the array is ideally rigid, phase accuracy will still be limited by guiding errors of the master telescope. Let us take all the same parameters as in § 2.2.2., except that an 0.13 arc sec Airy-disk replaces the 1 arc sec seeing disk, and T_c is increased to 100s: we find a RMS error of about 1 marc sec for a magnitude-15 object. For fainter objects, tracking the whole-array fringe signal becomes a better approach, perhaps the only one; of course this no longer works if the object is fully resolved.

The next solutions are far more complex, and would probably appear only in a second-generation array. First, we can guide on reference stars in the field of the master telescope; we need at least two in order to check the spinning itself. Having a sufficiently aplanatic master telescope is no trifle; furthermore, we must also de-spin the whole focal-plane assembly of guiding detectors, in order to keep them on the stars. Then, transmitting the G-control laser beams to the slave telescopes becomes arduous. Second, we can track fringes from reference stars (as discussed in Ref 5), with several fibers *and* delay lines, which is even more complex. All these difficulties have nothing to do with our specific proposal, and will appear in any type of array, particularly if it is spinning.

Which means we should consider gyroscopes. Performance expected from the Stanford Gravity-Probe experiment (Ref 10) must be quoted here. In order to measure very small relativistic effects, the angular shifts between a small orbiting telescope pointing at a star, and a set of superconducting spinning balls will be measured. Here we may have such a gyroscope similarly connected to our master telescope; after initial acquisition of the astronomical object, our master guider is no longer operated from the object photons, but from the gyroscope signals; the rest of the G-control is unmodified. The first essential limitation is angular drift, which increases with time; Stanford goal is 0.1 m arc sec/year, considerably better than we need. The second and more serious one is noise from the gyro readout device (based on SQUID detectors and the London-moment of the balls), which decreases with integration time; a figure of 1 m arc sec in 2 h is so far quoted as achievable, roughly equivalent to guiding on a magnitude-11 star in our above example. At the cost of dropping rigorous spherical symetry of the rotor (which would increase drift), a lower-noise optical readout may perhaps be developed.

4. PROOF-OF-CONCEPT

Before our ground or space arrays are seriously proposed, we want to carry out two separate low-cost demonstrations. The first is experimental: mounting two very small telescopes on a radio dish. The second is a numerical simulation of the complete array.

4.1. Experimental

First, more laboratory tests of fibers, and in particular more *quantitative* ones are needed: one must establish the practical bandwith limit for a given fiber-pair in different spectral ranges, and demonstrate the measurement of *accurate* visibilities irrespective of guiding

errors (Ref 6). In a second stage, one might try the §2.5 detection schemes.

The main program should be astronomical. We must show that usable fringes can indeed be observed with fibers from two telescopes, and we also want to demonstrate all the control techniques needed for our proposed arrays. As in Ref 21, we shall work in the 600 to 900 nm range with SiO2 fibers, and PM's and CCD's as detectors, and use 20-cm so-called Schmidt-Cassegrain amateur telescopes, with slight modifications. We need a pair of fast guiders, similar to that in Ref 4. The full G-control system must be built. The tests involve four steps: a) in the laboratory, in front of a collimator; even so, vibrations and air turbulence may already be added; b) the telescope pair is mounted on a small equatorial drive, and tested on some of the brightest red stars; base length is increased up to about 2 m; c) the pair of optical fibers (with the mixing platform, but without the telescopes) is taken to a radio dish and tested with internal light sources, as in Ref 21; results will show if passive protection is adequate, and if not, the I-control must be added; d) the complete system is put on the dish, and base length increased to the full diameter; fainter unresolved stars must now be used. At a later stage, fringe tracking could be added.

Lastly, one should compare seeing and IR transmission at likely radio-dish sites.

4.2. Numerical simulation

The array can be simulated by existing programs such as AIPS (from NOAO), or the Caltech VLBI package. These will require only slight modifications regarding the input format for the visible and NIR cases. These modifications reflect the fact that we are dealing with a fringe intensity pattern as opposed to amplitudes and phases in the radio case. Also, image reconstruction can be simulated using programs from these packages such as CLEAN, self-calibration, maximum entropy, or combinations thereof. The input to these programs will include the effects of various residual phase errors, when these become known. Two distinct simulations have to be performed: the space phased array, and the ground-based coherent array.

The results should indicate optimal baselines and size of the telescopes with respect to ease of image reconstruction and UV coverage. Such simulations have been conducted by others at different levels (Ref31), and we intend to gain fully from past experience.

5. CONCLUSION

The use of single-mode fibers constitutes a new approach to the construction of telescope arrays, which reduces many of the practical problems at the cost of a restriction in the spectral range. Mounting the array on a radio telescope gives a further important simplification, while limiting the base-length. Even so, the full project is a large scale one, but a low-cost proof-of-concept demonstration of the main technical points is feasible. Because several of the proposed solutions are novel, many new difficulties must be expected. Some other major remaining uncertainties are the actual amount of astrophysical work open to a many-small-telescopes array with maximum baselines of the order of 40 m, and the suitability of seeing at potential radio sites.

Acknowledgments. For permission to use the Hat-Creek radiotelescope, we thank J. Welch, and D. Cudaback who also gave great help in performing the tests. At Owens Valley, the operation was made possible by the interest of M. Cohen, and H. Hardebeck helped on the spot. P. Connes thanks J. Beckers for an invitation to NOAO-ADP, J.Breckinridge and S. Synnott for one to JPL, and M. Poulain for discussing IR fibers.

6. REFERENCES

1. Boudon Y & al 1978, Rech Aerospatiale, 6, 335
2. Coccoli J 1984, IEEE Trans Aerosp El Syst, AES 20,428; Chow & al 1985, Rev Mod Phys, 57, 61
3. Connes J & al 1967, Jour Phys, Coll C2 28, 120
4. Connes P & Michel G 1975, App Opt 14 2067
5. Connes P, Froehly C, Facq P 1984, ESA SP 228,49
6. Connes P, Roddier F, Shaklan S 1987, ESO-NOAO Oracle Workshop, 165

6A. Connes P, presented at Technical Working Group Meeting "Optical Interferometry in Space", JPL, March 30-31 1986

7. Davis J 1986, Nature, 323, 234
8. Davis D & al 1980, App Opt 19, 4138
9. Dandridge A & al 1984, J Lightw Tech, LT2, 73
10. Everitt C & al, 1983,"The GP-B Relativity Gyroscope Experiment", W Hansen Lab Internal Report, Stanford University. See also 7 papers in SPIE 619, 27 to 164, 1986
11. Froehly C 1981, ESO Conf "High Angular Resolution" (Garching), 285
12. Greenaway A, 1982, Opt Comm, 43, 157.
13. "Hinds International Inc" Technical Catalog, Type JCK modulators.
14. Koechlin L 1984, Thèse, Université de Nice
15. Labeyrie A 1975, Astrophys J Lett 196, L71
16. Labeyrie A 1987, ESO-NOAO Oracle Workshop, 97
17. "Le Verre Fluoré" Technical Catalog (St Erblon, 35230, France)
18. Mariotti J 1984, IAU Coll 79, (Garching), 257
19. Miyashita T 1982, IEEE J Qu Elect, QE 18, 1432.
20. Roddier F 1983, Adv Space Res, 2, 3; Roddier F, Breckinridge J 1984, Bull Am As Soc 16, 382
21. Roddier F & Shaklan S 1987, App Opt 26, 2159
22. Roddier F & Shaklan S 1986 NOAO Report 86
23. Roddier F & Lena P 1984, J of Optics 15, 171,363
24. Roddier F 1986, ESO VLT Report 49, 55
25. Roddier F & Roddier C 1986, SPIE 628, 298
26. "York Technology LTD" Technical Catalog, (Princeton NJ 08540, USA)
27. Saulson P 1984, Rev Sci Inst, 55, 1315; Karim M 1984, J Sci Inst, 55, 103; Rinker R & Faller J 1984, Nat Bur Stand Spec Pub 617, 411
28. Shao M & al 1984, Bull Am As Soc 16, 750
29. Shao M 1980, App Opt, 19, 1519
30. Stone J & Marcuse D, 1986, J Lightw Tech, LT4,
31. Stachnik R & al 1984, ESA SP 228, 35; Noordam J & al, ibid, 63; Faucherre M & al, ibid, 121; Lacasse M & al, ibid, 133; Hofman K & al, ibid, 145; ESO VLT Report 49, Appendix A2.
32. Staff of Space Department 1974, J Spacecraft, 11, 637
33. Swanson P & al, 1986, Opt Eng, 25, 1045
34. Townes Ch & al 1978, ESO Conf "Optical Telescopes of the Future"
35. Thomson A & al 1980, Astrophys J Supp, 44, 151
36. Tran D 1984, J Lightw Tech, LT2, 566
37. Ridgway 1987, ESO-NOAO Oracle Workshop, 245
38. Lu G & Aggarwal I 1987, 4th Int Symp Halide Glasses, 21
39. Wehr M & Le Sergent C 1986, SPIE 618, 130
40. Kimura M & al. 1986, SPIE 618, 85